Mineralogical Magazine, October 2003, Vol. 67(5), pp. 967–987

Using neutron diffraction measurements to characterize the mechanical properties of polymineralic rocks

P. F. SCHOFIELD[1,*], S. J. COVEY-CRUMP[2], I. C. STRETTON[3], M. R. DAYMOND[4], K. S. KNIGHT[4,1] AND R. F. HOLLOWAY[2]

[1] Department of Mineralogy, Natural History Museum, Cromwell Road, London SW7 5BD, UK
[2] Department of Earth Sciences, University of Manchester, Oxford Road, Manchester M13 9PL, UK
[3] Bayerisches Geoinstitut, Universität Bayreuth, Bayreuth, D-95440, Germany
[4] ISIS Facility, Rutherford Appleton Laboratory, Chilton, Didcot, Oxon OX11 0QX, UK

ABSTRACT

Conventional experiments designed to investigate the mechanical properties of polycrystalline geological materials are generally restricted to measurements of whole-rock properties. However, when comparing the measurements with theoretical models, it is frequently essential to understand how the deformation is accommodated at the grain-scale. This is particularly true for polymineralic rocks because in this case most theories express the whole-rock properties as some function of the properties of their constituent minerals, and hence the contribution which each phase makes to those properties must be measured if the theories are to be fully assessed. The penetrating nature of neutrons offers a method of addressing this problem. By performing deformation experiments in the neutron beam-line and collecting neutron diffraction patterns at different applied loads, the lattice parameters of all the mineral phases present may be determined as a function of load. The elastic strain experienced by each phase is then easily determined. Moreover, the strain in different lattice directions is also obtained. From this information a wide range of problems relevant for the characterization of the elastic and plastic deformation behaviour of polymineralic geological materials can be explored. An experimental technique for carrying out such experiments is described, and its validity is demonstrated by showing that the results obtained from deforming an elastically isotropic olivine + magnesiowüstite sample agree, to within very tight bounds, with the behaviour predicted by theory for elastically isotropic composites.

KEYWORDS: neutron diffraction, mechanical properties, polymineralic rocks.

Introduction

ONE of the major aims of experimental rock mechanics is to develop and evaluate constitutive equations which describe the elastic and crystal plastic properties of geological materials. Measurements of elastic properties play a central role in attempts to use seismological data to refine our understanding of the structure and composition of the Earth's interior, while measurements of plastic properties are used in geophysical models of the large-scale thermo-mechanical evolution of the lithosphere. The lithologies of interest in these applications are predominantly polymineralic composites which have mechanical properties that are a strong function of composition and microstructure. The range of compositions and microstructures which are encountered in natural rocks is too large for it to be feasible to determine the properties of every interesting rock-type individually. However, the number of volumetrically significant rock-forming minerals is small, and there is no *a priori* reason for thinking that the number of significant microstructural variables is large. Consequently, although experimental programmes designed to measure the mechanical properties of 'representative' rock-types are still

* E-mail: p.schofield@nhm.ac.uk
DOI: 10.1180/0026461036750138

performed, increasingly attention is being devoted towards finding more generic descriptions in which the properties of the polymineralic material are presented as some weighted sum of the properties of the constituent phases, with the microstructural variables added as a parameterization of the equations.

Several theoretical approaches to the problem of predicting the properties of composite materials in terms of those of their constituent phases have been developed (e.g. for elastic properties: Watt *et al*., 1976; Willis, 1981; Hashin, 1983; Nemat-Nasser and Hori, 1999; Zheng and Du, 2001; and for plastic properties: Fan and Miodownik, 1993; Zhao and Ji, 1997; Ponte Castañeda and Suquet, 1998). For the experimentalist seeking to test this theoretical work and guide its further development, the key requirement is to be able to measure the contribution which each constituent phase makes to the whole-rock properties. However, in typical rock-deformation experiments it is generally only whole-rock properties that can be measured. At large strains, knowledge of how each phase contributes to the bulk properties may be ascertained by examining the deformation microstructure after the experiment to establish how the strain has been partitioned between the phases. However, this is less easy at small strains where the deformation-induced microstructural changes are correspondingly smaller, and it is impossible for purely elastic deformation which is, by definition, completely recovered upon unloading. The resulting gap between the theoretical and experimental work has proved to be a particularly intractable one to solve.

Neutron diffraction experiments conducted on samples held under differential load within the neutron beam potentially offer a solution to this problem. If neutron diffraction patterns of sufficient quality can be obtained from a polymineralic sample held under an applied differential load, then the lattice parameters of each of the constituent phases may be determined at that load. By monitoring the change in these lattice parameters with load, then the average elastic strain experienced by each constituent phase may be determined as a function of load. From this information the contribution which each phase makes to the whole rock elastic properties is given. Moreover, if the elastic properties of each phase are known, then the stresses experienced by each phase may be determined from the elastic strains. Hence, given knowledge of the stress/total strain behaviour of each phase the contribution which each phase makes to the whole-rock deformation when the sample is deforming plastically may be ascertained. In principle, X-rays may also be used in this way. However, the penetrating nature of neutrons, which is typically several orders of magnitude greater than for X-rays of comparable wavelength, means that with neutrons the experimentalist is not restricted to working with tiny samples or to looking at near-surface regions of the sample, and therefore can avoid the difficulties associated with interpreting mechanical data under such circumstances.

Neutron facilities equipped to carry out uniaxial deformation experiments in the neutron beam-line include EPSILON on beam-line 7A of the pulsed reactor IBR-2 at the Joint Institute for Nuclear Research in Dubna, Russia, SMARTS at the LANSCE spallation source, Los Alamos National Laboratory, New Mexico, USA, and ENGIN at the ISIS neutron spallation source in the UK. Historically, the deformation experiments which have been carried out at these facilities have been concerned primarily with investigating the development of internal elastic strains within engineering materials (e.g. Dunand *et al*., 1996; Daymond *et al*., 1999*b*; Carter and Bourke, 2000), and with developing a technique for investigating local variations in strain within engineering components (e.g. Daymond *et al*., 1997; Webster and Ezeilo, 1997). Such experiments are becoming more widely performed, but with the exception of a recent study of the elastic behaviour of some quartz-rich sandstones (Frischbutter *et al*., 2000), and of the variation in strain at different locations within a sample of a calcite marble loaded in compression (Meredith *et al*., 1997), none has been performed on geological materials. In contrast, there is a much longer history of using neutron diffraction to determine the magnitude of mechanically and thermally induced residual elastic strains in engineering materials (e.g. MacEwen *et al*., 1983; Majumdar *et al*., 1991) and in monomineralic geological materials (Scheffzük *et al*. 1998; Pintschovius *et al*., 2000; Meredith *et al*., 2001). In addition to the facilities named above, such residual strain measurements are made on the E3 beam-line of the Hahn-Meitner Institute (HMI) in Berlin, the REST beam-line at the Studsvik Neutron Research Laboratory in Sweden, the high flux D1A beam-line at Institute Laue-Langevin (ILL) in France, and by the ANDI group at Chalk River

Laboratories in Canada. A more detailed description of all of these facilities and their potential for studying geological materials is provided by Schäfer (2002).

In this paper, we describe an experimental technique, developed on the ENGIN beam-line (Johnson *et al.*, 1997) of the ISIS neutron spallation source, Rutherford Appleton Laboratory, UK (Wilson, 1995), to investigate the mechanical properties of geological materials using the type of experiment described above. We demonstrate the validity of the technique using a simple analysis which permits experimental measurements of the strain partitioning between the phases in an elastically isotropic olivine + magnesiowüstite composite to be compared with widely accepted theoretical predictions of the elastic properties of isotropic composites. The technique is particularly well suited for addressing the geologically important concerns associated with obtaining a detailed quantitative understanding of the factors which control the elastic anisotropy and the plastic yield behaviour of both monomineralic and polymineralic geological materials. The results of experiments designed to explore both of these last two ideas are reported elsewhere (Covey-Crump *et al.*, 2003*a*,*b*). However, the potential of the technique for addressing these and other problems in the field of experimental rock mechanics is outlined.

Experimental details

The ISIS facility and the ENGIN beam-line

ISIS is a pulsed, time-of-flight neutron spallation source in which the neutrons are produced by bombarding a heavy-metal target with high-energy particles. In this process, H^- ions are accelerated in a linear accelerator, converted into protons, and then injected into a proton synchrotron ring, where they are further accelerated to 800 MeV. Fifty times a second, the protons are extracted from the synchrotron and fired into a tantalum metal target. The collisions between the protons and the tantalum nuclei induce cascade reactions within the nuclei which result in the release of neutrons with a wide range of energies. The energies of these neutrons are very high, and are reduced to usable values by passing them through hydrogenated moderators (water, liquid methane, or liquid hydrogen) where they undergo repeated collisions with the hydrogen nuclei. The exact spectral properties of the neutrons emerging from the moderator with each pulse (Fig. 1) are fixed by the temperature, composition, and size of the moderators. On either side of the target station are a series of beam-lines leading to neutron scattering instruments which are designed to exploit the advantages of the high flux, brightness, spectral range, and polychromatic nature of the pulsed neutron beam. The positions and distances of these instruments relative to the target station are integral in defining the flux and wavelength characteristics of the neutron beam which interacts with the sample.

In order to measure the elastic strains within geological materials at a resolution sufficient to be interesting, there are three essential requirements. Firstly, the beam must be of sufficiently high flux to penetrate samples several millimetres or more in size. Samples of this size are required to avoid the large stress heterogeneities which arise near to the free surfaces/ends of the sample during loading from the constraints imposed by the geometry of the specimen/apparatus assembly. Secondly, a medium/high resolution diffractometer capable of measuring strains to a high precision in minerals which may be both structurally similar and of considerable crystal chemical complexity is required. Thirdly, the working environment must be sufficiently large to accommodate the load frame and any other experimental equipment. All three requirements are satisfied on the ENGIN instrument at ISIS. This instrument is located only 15 m from the target, and was designed specifically for performing non-destructive strain scanning experiments on large engineering components under realistic engineering conditions of stress and temperature.

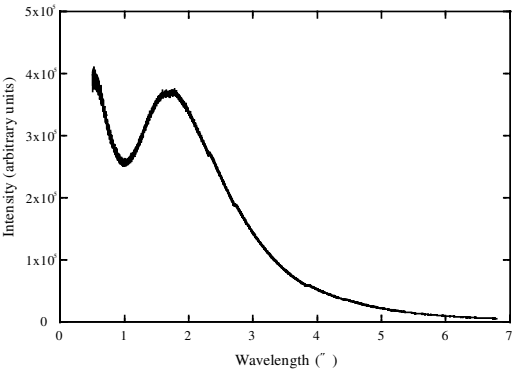

FIG. 1. The flux-wavelength distribution of neutrons produced from a tantalum target with a liquid methane moderator, as measured by a neutron scintillator detector 11.6 m from the moderator.

On ENGIN, the neutron diffraction patterns are collected as time-of-flight data in two, fixed detector banks located at ±90º to the incident beam. The polychromatic nature of the incident neutron beam means that for a material composed of grains with random orientation, a pattern containing many diffraction peaks is collected in each detector bank (Fig. 2*a*), in a manner analogous to energy dispersive X-ray measurements. The *d* spacings of the lattice planes which are oriented correctly for diffraction are obtained from the time-of-flight data by combining de Broglie's equation,

$$\lambda = h/mv = ht/mL \qquad (1)$$

where λ is the wavelength of the incident neutron, h is Planck's constant, m is the mass of a neutron, v is the velocity of the neutron, t is the time-of-flight of the neutron, and L is the length of the flight path, with Bragg's equation,

$$\lambda = 2d_{hkl} \sin\theta \qquad (2)$$

where d_{hkl} is the d spacing of the hkl plane and θ is the angle of incidence of the diffracted neutron on the hkl plane, to give,

$$d_{hkl} = ht/(2mL \sin\theta) \qquad (3)$$

Since the experiment is performed with a fixed geometry (i.e. a fixed angle of 2θ), then the scattering vectors of all the diffracted neutrons collected by a given detector lie in the same direction relative to the sample. Moreover, since the material is polycrystalline, provided that there are sufficient grains present in the measurement volume, the experiment mimics a powder diffraction experiment, i.e. each diffraction peak is produced from neutrons which have been diffracted from a number of different grains, each oriented such that the Bragg condition is satisfied. A diffraction pattern with a d spacing coverage of 0.4–3.3 Å at a resolution of $\Delta d/d = 0.7\%$ is collected for each pulse of neutrons, and these patterns are recorded over an extended period and summed to produce the final data set.

In order to reduce the data collection time, each detector bank on ENGIN is in fact composed of three rows of forty-five detectors encompassing an angular range of $83º < 2\theta < 97º$ (Fig. 2*b*). This increases the neutron detector solid angle coverage and so maximizes the counting statistics. In such a detector bank, each individual element is at a unique angle $2\theta = (90-x)º$. Hence the lattice parameter d_{hkl} occurs at a slightly different time in each detector (equation 3) and the diffraction patterns collected by each individual detector must be focused (shifted in time) to an effective scattering angle of $2\theta = 90º$ before they can be summed together (Johnson, 1988). The parameters required for this focusing are determined by calibrating the instrument using standard powders. Although the final diffraction data are focused to reflect a single scattering angle of $2\theta = 90º$, it should be noted that the final diffraction pattern remains a sum of all the scattering vectors coincident with the detector

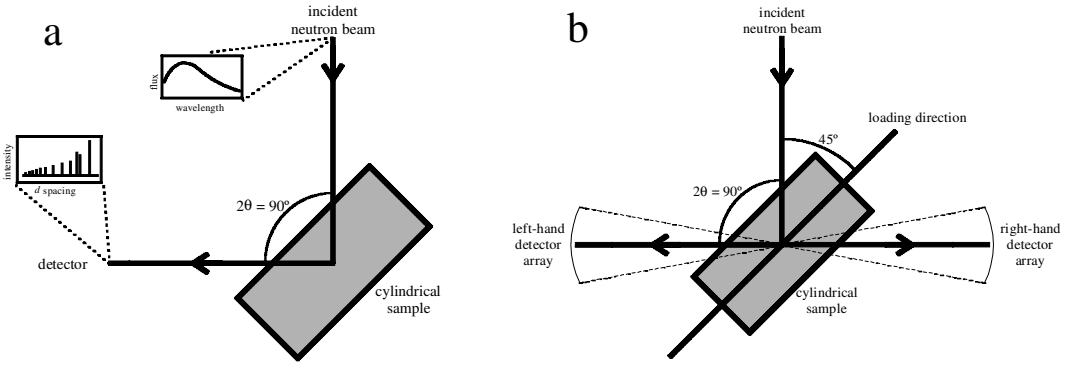

FIG. 2. Plan view, schematic representations showing the geometry of the incident beam, sample, and detector arrays on the ENGIN beam-line. (*a*) With a polychromatic neutron beam incident upon a sample containing a random orientation of grains, a diffraction pattern is collected with each pulse of neutrons by a detector set at fixed angle with respect to the incident beam. (*b*) The basic geometry of the experiment on ENGIN with the sample mounted horizontally in the loading frame and positioned with the loading axis at 45º to the incident beam. Two detector banks, with a fixed scattering angle of $2\theta = 90º$ and an angular coverage of $83º < 2\theta < 97º$ are located, one either side of the sample.

bank (±7º). This means that diffraction data collected by a single detector at a $2\theta = 83º$ come from a different set of lattice planes than the data collected by a detector at a $2\theta = 97º$. While increasing the angular coverage of the detector bank does introduce a potential loss of directional resolution, Daymond (2001) has shown that for an angular coverage of up to $20º2\theta$, the 'blurring' induced into the final strain determination is negligible across the d spacing range covered.

Experimental procedure

The experimental samples are right-circular cylindrical cores. These are loaded in compression, at room temperature (20ºC), in a 50 kN hydraulic Instron load frame (Daymond and Priesmeyer, 2002) positioned such that the loading axis is horizontal and at 45º to the incident beam. The sample is initially taken to a small load (typically 0.1 kN) and held at that load while the neutron diffraction data are collected. Once a diffraction pattern of sufficient quality has been obtained, the sample is taken to a different load and held there while a further set of neutron diffraction data is acquired. This procedure is repeated until neutron diffraction patterns from a desired number of loads have been obtained. Throughout the experiment, the applied load and apparatus crosshead displacement are monitored. In addition, for samples which are taken beyond their elastic limit, the bulk strain parallel to the loading direction is monitored using a capacitance extensometer attached to the sample. The experimental loading is controlled by, and integrated with, the data acquisition process.

The geometry of the experiment (Fig. 3), with the loading axis at 45º to the incident beam and the detectors at ±90º, is chosen so that the detector bank to the right of the sample records neutrons diffracted from lattice planes perpendicular to the loading direction (i.e. with scattering vectors parallel to the loading direction), and so records the component of strain in the constituent mineral phases which is parallel to the loading direction (hereafter referred to as axial strains). Conversely, the detector bank on the other side of the sample records neutrons diffracted from lattice planes parallel to the loading direction (i.e. with scattering vectors perpendicular to the loading direction), and so records the component of strain in the constituent mineral phases perpendicular to the loading direction (hereafter referred to as radial strains). Thus the lattice parameters recovered from the diffraction pattern collected by a given detector are the mean lattice parameters parallel to the scattering vector as averaged over all the grains satisfying the Bragg condition for that detector in the sampling volume. Hence, for example, the a, b and c lattice parameters of a given mineral phase recovered from the diffraction pattern recorded in the detector oriented for axial strains, are the mean values of a, b and c parallel to the direction of loading. These issues are further described in Fig. 4.

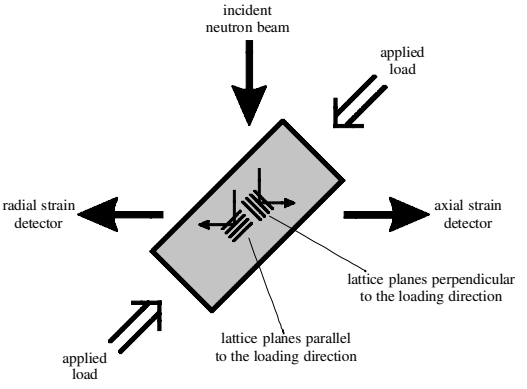

FIG. 3. Plan view of the experimental arrangement. This geometry permits the simultaneous collection, in the respective detectors, of diffraction data for which the lattice planes lie perpendicular to the loading direction (axial direction) and parallel to it (radial direction).

In the experiments used to develop this technique, samples 25 mm long by 10 mm in diameter have been used. This sample size was chosen to produce stresses close to the uniaxial compressive strength of the majority of geological materials at the 50 kN loading capacity of the Instron load frame, thereby permitting the maximum stress (and hence the maximum elastic strain) to be attained. Given a higher load capacity load frame, larger samples could have been used. However, for tests conducted in compression it is important to use samples with a length:diameter aspect ratio close to 2.5 because at smaller aspect ratios the stress heterogeneities generated by the friction at the sample/piston interfaces (Birch *et al.*, 1976) compromise the interpretation of the mechanical data, while at larger aspect ratios buckling forces become an issue (Cropper and Pask, 1969).

The maximum strains attainable in the experiments are limited by the onset of brittle

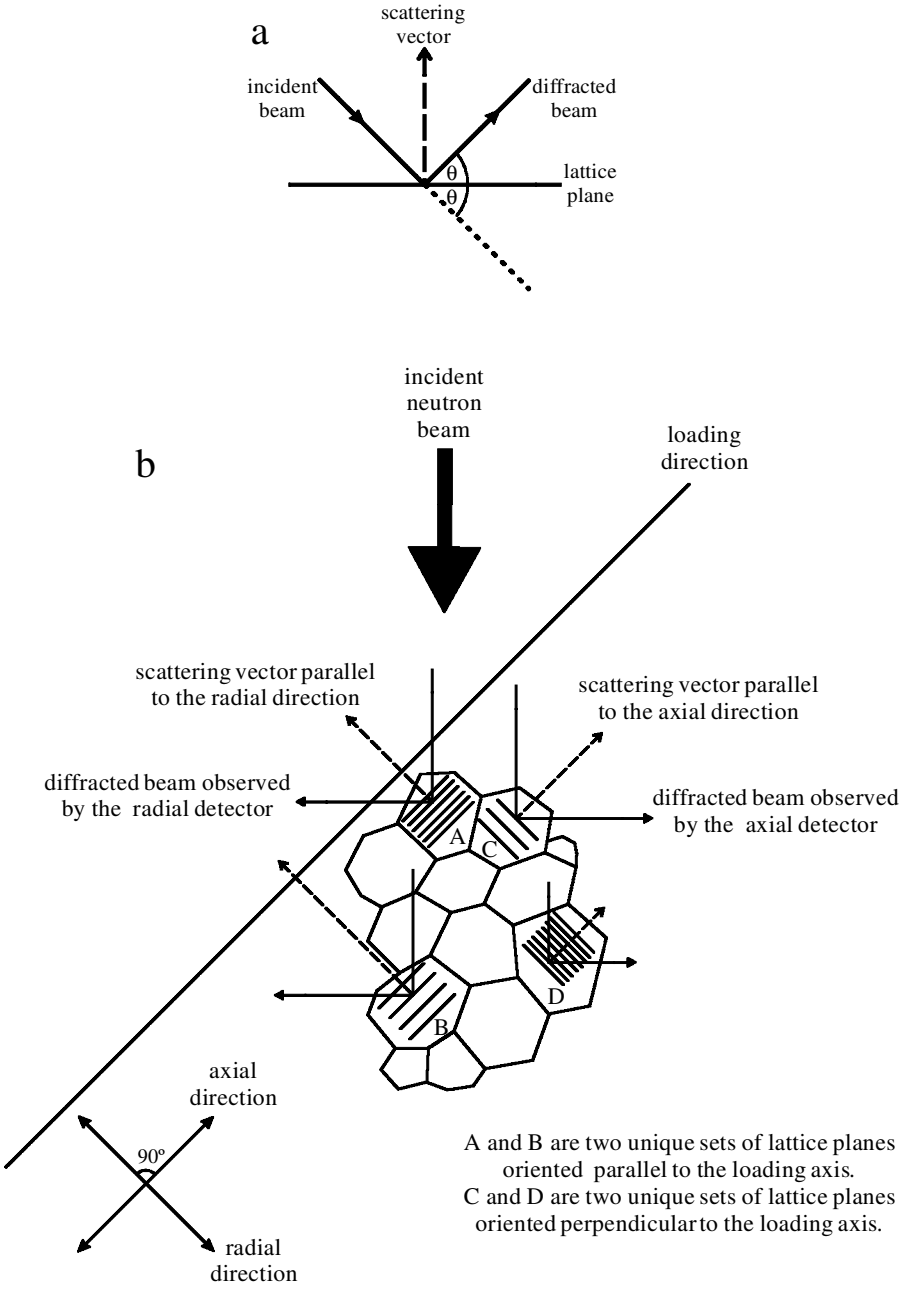

FIG. 4. (*a*) For an incident and diffracted beam inclined at an angle θ to the lattice plane, the scattering vector is normal to the lattice plane. (*b*) With the geometry such that the sample is horizontal and at 45° to the incident beam, and with two detector banks fixed at ±90° to the incident beam, only lattice planes with a scattering vector lying parallel to the radial direction of the sample (A and B) will diffract neutrons toward the radial detector bank. Lattice planes with a scattering vector lying parallel to the axial direction of the sample diffract neutrons toward the axial detector bank (C and D). Note that if the orientation of grains A and B are not the same, then the neutrons recorded in the radial detector bank are diffracted from a different set of lattice planes in A than they are in B. Similarly, for grains C and D.

deformation, which for almost all the volumetrically significant minerals is strongly favoured over crystal plastic deformation at room temperature and pressure. Typically, brittle failure of the samples occurs by a bulk strain of 1%, although samples in which one or more of the phases deforms plastically can be taken to larger strains.

The volume element (voxel) from which the data are collected should be as large as possible so that it is as representative of the sample as possible, by encompassing any heterogeneity in the spatial distribution of the mineral phases and by accommodating as many grains as possible. Numerical modelling of the mechanical behaviour of elastic-plastic materials (e.g. Daymond and Priesmeyer, 2002) suggests that around 1000 grains will produce results within a few percent of the value obtained from a much larger number of grains, although ideally 5000 grains should be incorporated (Clausen, 1997). Since a number of other neutronic issues typically limit the voxel dimensions to around $5 \times 5 \times 20$ mm, this suggests a maximum grain diameter for experiments of this type of approximately 1 mm. The voxel size is set by the sample diameter and the horizontal and vertical dimensions of the neutron beam. In the experiments described here this typically amounts to a volume element $2 \times 5 \times 10$ mm in size located at the centre of the specimen, and defined using an incident beam slit 5 mm wide and 10 mm high, with the outgoing beam defined using radial collimators to be 2 mm.

Data collection strategies

Given access to the facilities required to perform the experiments, the most important practical consideration is that of the time required to collect neutron diffraction patterns of the requisite quality. Clearly, the longer the data collection time, the better the quality of the diffraction data, the lower the uncertainty associated with the lattice parameters, and hence the higher the strain resolution of the experiments. However, access to neutron beam-time is in high demand, and within any allotted period of beam-time, measurements at several different applied loads are required. This time constraint has several significant consequences for the choice of experimental material. These consequences fall into two categories: mineralogical and mechanical. Among the mineralogical issues which bear consideration are the following.

(1) At what point does the complexity of the crystal chemistry of the minerals in the sample become too great for neutron diffraction patterns of the requisite quality to be obtained in a reasonable period? As symmetry decreases and crystal chemical complexity increases, so the complexity of the diffraction pattern increases. Moreover, as the unit-cell volumes increase, the absolute intensity of the diffraction peaks decreases. Increased complexity and decreased intensity in diffraction patterns both require longer data collection times. From the experiments performed to date, the length of time required to obtain a similar uncertainty on the unit-cell volume at given volume fraction of the phase in the sample, has been found to be: halite > orthopyroxene (En_{90}) > garnet > olivine (Fo_{90}) > calcite > quartz > anhydrite > magnesiowüstite (Mg_{80}). These amount to actual data collection times of the order of 2.5–3 h for halite and orthopyroxene, and 1–1.25 h for magnesiowüstite.

(2) At what point does structural similarity become a problem? Minerals with similar structures, for example ortho- and clinopyroxenes, possess inherently similar diffraction patterns. In such situations the diffraction peaks of the different minerals may overlap significantly. As the separation of the diffraction peaks decreases, so the data collection times must be increased in order to separate the contribution to the diffraction pattern from each phase and thus maintain the quality of the refined lattice parameters. Dealing with this issue requires the maximum possible resolution from the diffractometer.

(3) What is the minimum volume proportion of the minerals which it is practical to use? This is strongly influenced by the crystal symmetry and crystal chemistry of the constituent minerals and by the separation of the diffraction peaks. For a series of calcite:halite mixtures it was found that for a given count time, the errors on the calcite unit-cell volume doubled as the volume proportion was reduced from 40% to 30%. With a 27:73 mixture of orthopyroxene and olivine, the $\Delta V/V$ uncertainties were three times higher for the orthopyroxene than for the olivine. However, with a strongly scattering, high-symmetry mineral such as magnesiowüstite, extreme volume proportions of 10% and less are possible, provided that there is minimal peak overlap with the other constituent minerals.

(4) What, effectively, is the maximum number of phases which can be present in the sample? In principle, this is also a factor of the scattering

properties of the phases involved in the mixtures, but it is more strongly influenced by the increased possibility of overlapping diffraction peaks. Data analysis of high-resolution powder diffraction patterns becomes challenging when the number of phases increases above two, and given the current experimental capabilities of ENGIN, mixtures of three or more phases are likely to induce over-parameterization in the data analysis or require impractical data collection times.

(5) To what extent can minerals containing OH^- and H_2O be present in the sample? Hydrogen scatters neutrons incoherently, imparting a large background to the data and reducing the signal-to-noise statistics of the diffraction patterns. This is important if hydrous minerals are present in the sample, either as alteration products or as a phase of particular interest. For powder diffraction experiments, this issue can be circumvented by deuterating the sample (deuterium scatters neutrons coherently) but this is not possible for solid samples of natural rocks. This hydrogen/deuterium issue can be numerically demonstrated using the data of Sears (1992) with hydrogen and deuterium having coherent scattering lengths of −3.74 fm and 6.67 fm, respectively, and incoherent scattering lengths of 25.27 fm and 4.04 fm respectively. The experiments described here simply seek to obtain the lattice parameters of the constituent minerals, and assuming that the diffraction peaks are clearly visible above any enhanced background, these problems can be accommodated in the data analysis. Thus, while it is likely that these experiments could accommodate many common hydrous minerals (e.g. amphiboles, micas and possibly serpentine minerals) if the counting times were sufficiently high, minerals with a greater number density of hydrogen (e.g. chlorites, gypsum) are unlikely to be possible.

(6) To what extent can minerals containing neutron absorbing nuclei be present in the sample? Many nuclei are neutron absorbers, but while strongly absorbing nuclei such as ^{113}Cd, ^{10}B, and many rare earth element isotopes are unlikely to be encountered in the volumetrically significant mineral phases, other isotopes such as ^{35}Cl which also possess absorbing characteristics, are present (e.g. in halite). As is the case when hydrous minerals are present, the presence of these elements causes a reduction in the number of scattered neutrons, that is, a reduction in both the signal and the signal-to-noise ratio, and so this problem may be circumvented by lengthening the counting times.

(7) At what point does the strength of a lattice-preferred orientation become an issue? Any deviation from a truly random orientation of the grains in a sample significantly alters the relative intensities of the diffraction peaks. Generally, this can be accommodated within the data analysis, but for minerals which are weak neutron scatterers with only one or two strong diffraction peaks, preferred orientations may have a serious effect if the lattice planes associated with the most intense peaks are oriented away from the Bragg condition. This issue has not been explored in detail in these studies, but a method of dealing with preferred orientations through the data analysis is described below.

Among the mechanical issues which bear consideration are the following.

(1) What mechanical property contrast between the minerals is required to obtain useful results in reasonable time? Experiments such as those described here may be performed upon monomineralic materials. However, if the goal is to study the properties of polymineralic materials, the mechanical property contrast between the minerals needs to be considered. From the experiments which have been conducted so far, a contrast of $E_1/E_2 > 1.1$ (where E_1 and E_2 are the Young's moduli parallel to the loading direction, of the stiffer and the more compliant mineral phases, respectively) proves to be sufficient for obtaining results which can be compared with a range of theoretical analyses of the elastic properties of polymineralic materials.

(2) To what extent do strain heterogeneities within the measurement volume cause problems? Strain heterogeneities may exist at the grain scale, i.e. grains in different orientations may be strained by different amounts, and they may exist at the scale of the sample, that is, they may be imposed during loading by the geometry of the sample/piston assembly. Such heterogeneities have the consequence that the lattice parameters of different grains of a particular mineral vary within the volume element seen by the neutrons. The result is peak broadening, and a subsequent loss in resolution in the diffraction pattern. Sample-scale heterogeneities may be avoided or minimized by decreasing the size of the voxel and/or locating the voxel in an area of the sample in which the deformation is homogeneous. Grain-scale strain heterogeneities are unavoidable: indeed these heterogeneities form the essence of

the problem which the experimental technique is designed to investigate. They are primarily responsible for the reduced quality of the diffraction patterns obtained in the experiments in comparison to those which would have been obtained from powdered samples of the same material on the same experimental station. Prior to the first experiment, the possibility that grain-scale heterogeneities would undermine the whole technique was a significant concern. However, for all materials so far investigated, this concern has proved ill-founded.

(3) To what extent can brittle or plastic deformation occurring during the neutron counting be tolerated? In brittle materials, at loads approaching the uniaxial compressive strength of the sample, sub-critical microcracking during the neutron counting period may occur. This is unimportant (unless it leads to macroscopic failure of the sample) because what is being measured via the neutron diffraction are the lattice strains and, at the scale of the volume element interrogated by the neutrons, these are significantly modified only if the fracture density is very high. In materials which deform plastically, greater problems are presented for the analysis of neutron diffraction patterns if the loads at which the neutron data are collected are above the elastic limit of any of the minerals present. Under such circumstances, the neutron counting takes place while the sample is deforming in what amounts to a conventional constant load creep test, and consequently, while the texture of the deforming phases, and possibly also the stress (and hence elastic strain) distribution between the minerals, is changing. These problems can be minimized by partially offloading the sample prior to neutron data collection, but this introduces other complexities for the interpretation of the plastic response. An alternative strategy is to shorten the period of neutron counting and to adjust the analysis of the results to accommodate the larger errors on the lattice parameters which thereby arise. An investigation of the loss of lattice parameter accuracy with decreasing neutron counting time for a plastically deforming garnet + halite sample, showed that reducing the count time from 150 to 30 min doubled the uncertainties in the unit-cell volume ($\Delta V/V$). However, importantly, despite a doubling in the magnitude of the error bars, there was no deviation from the underlying strain trends established by the data collected from the longer count times.

The combination of high flux, time-of-flight neutrons with good resolution, fixed geometry diffractometry, as is available on ENGIN, enables these experiments to be performed in realistic time scales. A simple quantitative analysis of how count times vary for a required uncertainty in peak position in the presence of a significant background is given by Withers *et al.* (2001). By combining data collection strategies, tailored to meet the requirements of the samples, their constituent minerals, and the ultimate goals of the study, sufficient data can be collected within the standard 2–4-day beam-time allocations. Moreover, the data analysis methods are extremely sophisticated, and many of the negative influences upon the diffraction data, such as the increased backgrounds arising from the presence of significant hydrous components, or the presence of strong textures, may be accounted for within the data analysis. Furthermore, a new beam-line, ENGIN-X (Johnson and Daymond, 2002), which will provide an order of magnitude improvement in count-rates compared to ENGIN was made available in Summer 2003.

Analysis of the neutron diffraction data

Elastic deformation changes the spacing of the lattice planes. These changes are manifested in the neutron diffraction data by lateral shifts of the associated diffraction peaks. Since the entire diffraction pattern is collected with each pulse of neutrons, it is natural to use whole-profile fitting methods to refine the data. This analysis is performed using the GSAS (General Structure Analysis System) code of Larson and Von Dreele (1994). A complete description of these analysis techniques is given in Young (1993), while the applicability of these refinement procedures for the measurement of lattice strains is discussed by Daymond *et al.* (1997, 1999*a*).

In whole-profile fitting methods of diffraction data analysis, non-linear least squares refinements are performed until a best fit is achieved between the entire measured diffraction pattern and the entire calculated diffraction pattern. The calculated patterns are based upon the simultaneously refined models of crystal structure, diffraction optics, sample dependent effects and instrumental parameters. Internally calculated shifts are applied to the initial parameters with the aim of producing an improved model, and the procedure is repeated. The resultant best least-squares fit is optimized by minimizing the residual, and

represents the best fit to the entire diffraction pattern, incorporating every data point. Importantly for this work, these profile fitting methods may refine multiple phases simultaneously, and additionally provide an accurate phase quantification from the actual volume element observed by the detector, a feature which is important for rocks that are microstructurally inhomogeneous.

If the crystal structures of the constituent phases are known, then the positions and intensities of the diffraction peaks can be predicted. Performing Rietveld analysis, a least-squares fit between the observed and predicted diffraction profiles, enables the atomic positions and the lattice parameters to be determined. Data for a specified time-of-flight range, usually from 3000–4000 μs to 19500–20000 μs are focused, background subtracted, normalized to the incident flux distribution, and then binned as $\Delta t/t = 0.0005$. This time-of-flight range is equivalent to a d spacing range of 0.5–3.5 Å in the ±90° detectors. The first refinement is performed on data collected at the lowest applied load with scale, background, phase fraction, lattice parameters, fractional coordinates, and atomic displacement factors all refined from those of the source data to produce a sample-specific seed-file which is used as the starting point for all subsequent refinements. The refinements of the diffraction data from each applied load are then performed in an identical fashion, with the same starting seed-file and the same parameters being varied each time. In addition to the parameters which are varied in the production of the seed file, the Gaussian strain broadening parameter for each phase is also varied when refining the data from the remaining loads. This is of particular importance in experiments where one of the two phases is yielding plastically, as the associated defects and strains induce a significant sample-dependent peak broadening. A typical diffraction pattern, its Rietveld refinement model, and the residual are shown in Fig. 5.

Powder diffraction and the normal Rietveld refinement procedure assumes that there is a random orientation of grains and that the grains are sufficiently numerous to present all possible orientations of lattice planes to the incident beam. However, in geological materials, both lattice-preferred orientations and large grain sizes are commonly encountered. When such is the case, the relative intensities of different diffraction peaks in the pattern may be altered significantly, as shown by the diffraction patterns in Fig. 6 which comes from a sample in which the lattice-preferred orientation is moderately well developed. When this effect becomes strong the

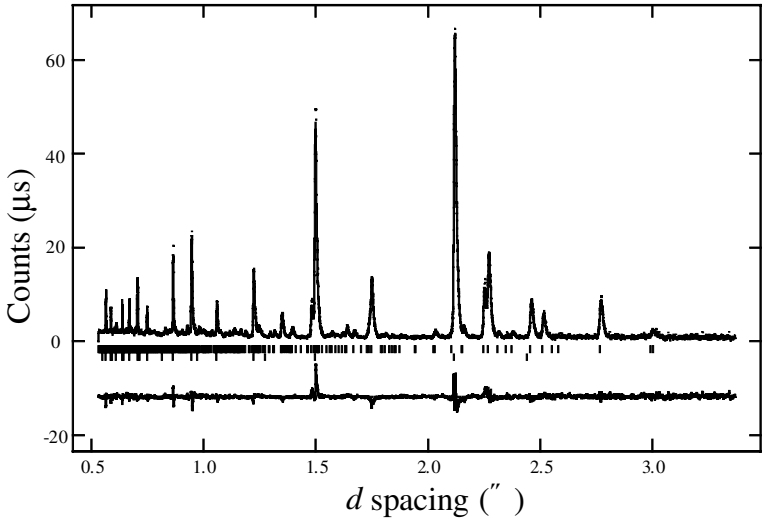

FIG. 5. A typical diffraction pattern obtained from an olivine + magnesiowüstite sample showing the calculated fit (top), and the resulting residual (bottom). The dots represent the diffraction data and the solid line represents the calculated profile. The ticks indicate the positions of diffraction peaks for olivine (top) and magnesiowüstite (bottom). The data shown are those obtained by the axial strain detector from a mixture of 54% olivine and 46% magnesiowüstite at 17 kN applied load.

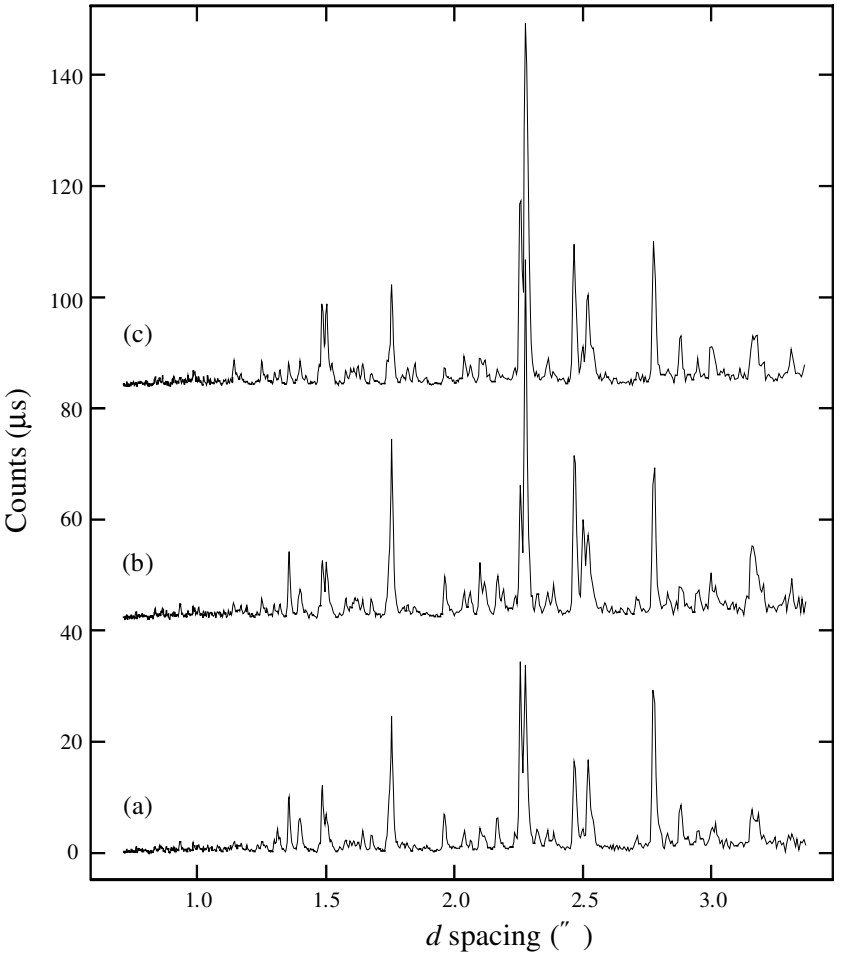

FIG. 6. Diffraction patterns taken from three orthogonally oriented samples cored from a single block of a 73% olivine + 27% orthopyroxene mylonite from the Oman ophiolite. The rock had a well developed foliation and a mineral elongation lineation within that foliation. There was a moderately well developed lattice-preferred orientation in both the olivine and orthopyroxene, the full details of which are given in Covey-Crump *et al.* (2003*a*). The loading directions in the three samples were (a) parallel to the lineation, (b) normal to the lineation but in the foliation plane, and (c) normal to the foliation plane, respectively. The effect of the lattice preferred orientation of the two mineral phases upon the diffraction patterns is evident from the differences in the relative heights of the diffraction peaks between each pattern. In each case the diffraction pattern was obtained at an applied load of 2 kN.

intensity distribution of the diffraction peaks is not well predicted by a basic Rietveld model. Two different routes may be used to circumvent this problem. Firstly, since the preferred orientations distort the diffraction peak intensities in a mathematically systematic manner, the effect can be accommodated by parameterizing the Rietveld model to approximate the observed preferred orientation. Some of the appropriate models for doing this are discussed by Wenk (1998). Alternatively, the effects of texture may be accommodated using a LeBail analysis. LeBail refinements differ from Rietveld refinements in being direct least squares fits to the observed diffraction profile. This procedure enables the lattice parameters to be determined by refining the peak positions while arbitrarily fitting the peak intensities. While the general analysis procedure is similar to that described above for a Rietveld analysis, fractional coordinates and atomic

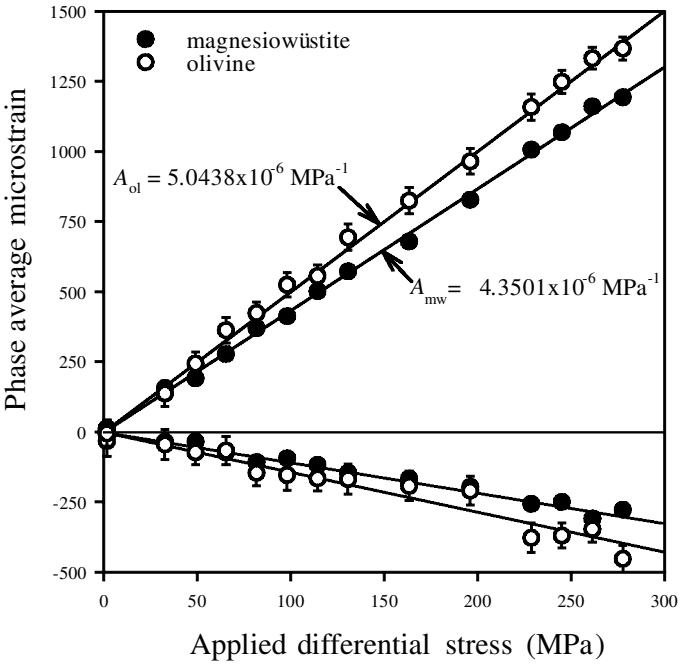

FIG. 7. The phase average strain in an elastically isotropic 54% olivine + 46% magnesiowüstite composite as a function of the differential stress applied to the sample. The phase average strain of each mineral is calculated directly from the measurement of the lattice parameters using equation 8. The strain behaviour of each phase is linear elastic, with compression in the axial direction being accompanied by extension in the radial direction. The elastically stiffer magnesiowüstite experienced less strain at given applied differential stress than the elastically more compliant olivine. Also shown are the best-fit curves to the data and the values of A (equations 16 and 17), i.e. the slopes of the axial strain/applied differential stress curve for each mineral phase.

displacement factors are not required (as they are primarily used to provide the peak intensities to the Rietveld model), and the phase fraction is not iterated beyond the preparation of the seed file. The two approaches work equally well in terms of obtaining an improved precision on the lattice parameters, except in the case of very poor quality diffraction data, when the more constrained process of parameterizing the texture is usually preferred.

The quality of the whole-pattern refinements can be assessed by direct observation of the fit and the residual, or from the following numerical agreement factors (Young, 1993) which are calculated with each refinement,

$$R_p = \Sigma|y_{i,obs} - y_{i,calc}|/\Sigma y_{i,obs} \quad (4)$$

$$R_{wp} = \{[\Sigma w_i(y_{i,obs} - y_{i,calc})^2]/[\Sigma w_i(y_{i,obs})^2]\}^{0.5} \quad (5)$$

$$R_{exp} = [(N - P)/\Sigma w_i(y_{i,obs})^2]^{0.5} \quad (6)$$

where y_i is the intensity at the ith point, $w_i = 1/y_{i,obs}$, N is the number of data points, and P is the number of parameters refined. R_p and R_{wp} are the pattern and weighted pattern agreement factors, and R_{exp} is the expected agreement factor. The 'goodness-of-fit' parameter (reduced χ^2) is the ratio $(R_{wp}/R_{exp})^2$.

Evaluating strains from the lattice parameters

The strain parallel to a given lattice direction w (e.g. a, b or c) in mineral phase x in direction y (axial or radial) at given load is obtained directly from the lattice parameters

$$\varepsilon_{w,x,y} = -\ln(w_{x,y}/w_{0,x,y}) \quad (7)$$

where $w_{0,x,y}$ is the lattice parameter evaluated at zero load. Since the experimental set up requires a small load to be applied to the sample to prevent the assembly falling apart (the sample is not gripped in any way), zero load measurements are not possible, and so the zero load value for each lattice parameter is obtained by least-squares fitting the load/lattice parameter data in the

elastic regime and extrapolating back to zero load. Determining the zero load values in this way is preferable to using literature values because it accommodates any residual strains which may be present in the starting material, as well as any crystal chemical differences between the actual minerals in the sample and those used to determine the literature values.

The strains parallel to given lattice directions are of importance for a wide range of applications of the experimental technique, but in problems in which the phase averaged properties are of interest, some measure of the phase average strains is necessary. The most convenient definition of the linear strain $\varepsilon_{x,y}$ in mineral phase x in direction y (axial or radial) at given load is

$$\varepsilon_{x,y} = -(1/3)\ln(V_{x,y}/V_{0,x,y}) \quad (8)$$

where $V_{x,y}$ is the apparent unit-cell volume of phase x, as given by the lattice parameters in direction y of that phase at that load, and $V_{0,x,y}$ is the zero load value of $V_{x,y}$. Once more, it is reiterated that since the lattice parameters are the average values of the lattice parameters in direction y, what is obtained from equation 8 are directional values of the phase average strain. The directional values of the phase average axial strain for an elastically isotropic sample are the same for all directions of loading relative to the sample, but this is not true for elastically anisotropic samples.

Some results

As an illustration of the results which can be obtained using this experimental technique, some measurements obtained from an elastically isotropic composite of 46 vol.% magnesiowüstite (Mg_{80}) and 54 vol.% olivine (Fo_{90}) are shown in Fig. 7. Full experimental details, a description of the material, and a tabulation of the results for this experiment, are given elsewhere (Covey-Crump *et al.*, 2001). In the experiment neither phase was loaded beyond its elastic limit, i.e. the deformation throughout the entire experiment was fully elastic. As expected, the behaviour of each phase was linear elastic, with compression in the axial direction being accompanied by extension in the radial direction. The elastically stiffer magnesiowüstite experienced less strain at given applied differential stress than the elastically more compliant olivine.

The errors on the strain measurements may be considered in various ways. Firstly, the errors on the lattice parameters, as determined from the fits to the neutron diffraction patterns, may be propagated through equation 8 and thereby converted into strains. The mean error in the phase average axial strain measurements obtained in this way for the olivine results shown in Fig. 7 is 43 μstrain (1 μstrain = 0.0001% strain). For the magnesiowüstite the mean error was 22 μstrain, although the real significance of errors less than ~40 μstrain, given the nature of instrumental uncertainties, is open to doubt. Nominal errors of less than 50 μstrain have been achieved for all the minerals that have been investigated so far. Such errors are over an order of magnitude better than those which are generally achieved in conventional uniaxial deformation experiments utilizing strain gauges attached to the sample. A second method of considering the errors is via the root mean square errors on fits to the phase average strain versus applied differential stress curve. These are typically significantly less than the errors arising from the lattice parameter uncertainty: the fit shown in Fig. 7 for the olivine axial strain results has a root mean square error of 22 μstrain. A third method of considering errors suitable for elastically isotropic materials, is to compare the Poisson's ratio obtained from the axial and radial strain results for given phase with the literature value. The Poisson's ratio ν_x of phase x is

$$\nu_x = -\varepsilon_{x,\text{radial}}/\varepsilon_{x,\text{axial}} = (\Delta\sigma_{agg}/\Delta\varepsilon_{x,\text{axial}})/(\Delta\sigma_{agg}/\Delta\varepsilon_{x,radial}) \quad (9)$$

The Poisson's ratios for olivine and magnesiowüstite using the best fit slopes shown in Fig. 7 are 0.286 and 0.246, respectively, which compare with the values obtained by isotropically averaging (using the Hashin-Shtrikman scheme) the single-crystal stiffness tensor for each phase, of 0.250 and 0.234, respectively. Given the sensitivity of the Poisson's ratio to the averaging schemes used to calculate it from the single crystal properties, this is good agreement.

Analysis of the results

The results of experiments such as those shown in Fig. 7 comprise a set of phase average strains for each mineral phase present in the sample at known applied differential stresses. The whole-rock strain at each applied differential stress is also known but much less accurately than the other variables. Consequently, the question

immediately arises of how best to make a comparison between the experimental results and theoretical models, given that in order to establish the contribution each phase makes to the total deformation it is important to know accurately what the total deformation is.

The following simple analysis strategy is strictly applicable only for the purely elastic deformation of elastically isotropic materials. For elastically anisotropic materials and for plastically deforming materials attention needs to be paid to the strains in the different lattice directions. However, the analysis may still prove useful for examining the pre-yield behaviour of plastically deforming materials, and, when the directional elastic properties of each phase are known, for examining the behaviour of elastically anisotropic materials, albeit if only to establish that the experimental results are consistent with first order theoretical requirements of material behaviour (see Covey-Crump *et al.*, 2003*a*).

General analysis strategy

When phase-averaged stresses and/or strains are known or are of interest in composites composed of mineral phases of similar grain size, a widely used starting point for the analysis of the mechanical properties is the rule of mixtures (e.g. Hill, 1963; Mecking and Dunst, 1994). For a two-phase composite this is

$$\sigma_{agg} = \phi_1\sigma_1 + \phi_2\sigma_2 \quad (10)$$
$$\varepsilon_{agg} = \phi_1\varepsilon_1 + \phi_2\varepsilon_2 \quad (11)$$

where ϕ_1 and ϕ_2 are the volume fractions of phase 1 and phase 2 respectively, and σ and ε are the phase averaged stresses and strains, respectively, of the subscripted phases (where agg refers to the whole-rock properties). Equations 10 and 11 may be derived from simple geometric considerations (e.g. Bloomfield and Covey-Crump, 1993). The simplistic nature of the rule of mixtures in weighting the contribution of each phase only by volume fraction without any regard for the role of microstructure (e.g. the spatial distribution of the phase in the material), is frequently noted (e.g. Clyne and Withers, 1993; Mecking and Dunst, 1994). However, the 'rule of mixtures' does have the advantage of being straightforwardly formulated in terms of the experimentally measurable variables and, moreover, it is frequently found to provide a reasonable description of elastic properties when only the Young's modulus is of interest.

In addition to the constraint equations supplied by the rule of mixtures,

$$\phi_1 + \phi_2 = 1 \quad (12)$$

and for purely elastic deformation

$$\sigma_{agg} = E_{agg}\varepsilon_{agg} \quad (13)$$
$$\sigma_1 = E_1\varepsilon_1 \quad (14)$$
$$\sigma_2 = E_2\varepsilon_2 \quad (15)$$

where the E are the Young's moduli of the subscripted phases. Equations 10 to 15 are the set of equations which must be solved to specify the system completely, i.e. to establish the values of all the stress and strain terms, and thereby to establish the contribution that each phase makes to the whole-rock properties.

The information supplied by the neutron diffraction experiments comes in the form

$$\varepsilon_1 = A_1\sigma_{agg} \quad (16)$$
$$\varepsilon_2 = A_2\sigma_{agg} \quad (17)$$

where the A are the slopes of the phase average axial strain *vs.* applied differential stress curves for the subscripted phases. Care needs to be exercised when combining this new information with equations 10 to 15 to ensure that both constraint equations 10 and 11 are utilized. Thus, substituting equations 13, 14 and 15 into equation 10, and then using equation 11 to substitute for ε_{agg} and rearranging,

$$\varepsilon_1/\varepsilon_2 = [\phi_2/\phi_1][(E_2 - E_{agg})/(E_{agg} - E_1)] = A_1/A_2 \quad (18)$$

where the equality on the right hand side of equation 18 follows from equations 16 and 17. Equation 18 permits the values of $\varepsilon_1/\varepsilon$ given by theoretical predictions of E_{agg} using known values of E_1 and E_2, to be compared with the neutron diffraction results through the measured values of A_1/A_2.

The value of E_{agg} compatible with the neutron diffraction measurements and stipulated values of E_1 and E_2 is given by rearranging equation 18,

$$E_{agg} = (E_1\phi_1A_1 + E_2\phi_2A_2)/(\phi_1A_1 + \phi_2A_2) \quad (19)$$

The values of E_{agg} obtained may then be compared directly with those predicted by theory. Alternatively, if there is confidence in the theory but E_1 or E_2 are poorly known, then by setting equation 19 equal to a theoretical expression which specifies E_{agg} in terms of ϕ_1, ϕ_2, E_1 and E_2, the poorly known value of E may be determined from the other E and the volume fractions using the neutron results.

Theoretical predictions of whole-rock behaviour

It may be shown on energetic grounds (Hill, 1952; Paul, 1960) that the elastic properties of composite materials are bounded by the conditions of homogeneous stress ($\sigma_{agg} = \sigma_1 = \sigma_2$) and homogeneous strain ($\varepsilon_{agg} = \varepsilon_1 = \varepsilon_2$). The homogeneous stress value of E_{agg} is readily obtained by substituting equations 13, 14 and 15 into 11, dividing through by $\sigma_{agg} = \sigma_1 = \sigma_2$, and rearranging,

$$E_{agg} = E_1E_2 /(\phi_2E_1 + \phi_1E_2) \quad (20)$$

Similarly, the homogeneous strain value of E_{agg} is obtained by substituting equations 13, 14 and 15 into equation 10, and dividing through by $\varepsilon_{agg} = \varepsilon_1 = \varepsilon_2$,

$$E_{agg} = \phi_1E_1 + \phi_2E_2 \quad (21)$$

It follows, therefore, that for purely elastic deformation, on a plot of ε_1 against ε_2, the neutron diffraction data must lie between the two curves of slope $\varepsilon_1/\varepsilon_2$ as given by equation 18 when using the homogeneous stress value of E_{agg} (equation 20), and the homogeneous strain value of E_{agg} (equation 21), respectively. If the data do not lie between these curves then either there is a problem with the experimental data or the values of E_1 and/or E_2 are incorrect.

For two-phase composites in which the constituent phases have very different elastic properties, the homogeneous stress and homogeneous strain bounds are widely separated, i.e. they provide a poor constraint on composite properties. Consequently, considerable effort has been devoted to deriving tighter bounds. Among the tightest bounds are those derived by Ravichandran (1994) under the approximation that the Poisson's ratios of both constituent phases are the same,

Bound 1:

$$E_{agg} = \{(cE_1E_2 + E_2^2)(1 + c)^2 - E_2^2 + E_1E_2\}/\{(cE_1 + E_2)(1 + c)^2\} \quad (22a)$$

Bound 2:

$$E_{agg} = \{[E_1E_2 + E_2^2(1 + c)^2 - E_2^2][1 + c]\}/\{(E_1 - E_2)c + E_2(1 + c)^3\} \quad (22b)$$

where $c = (\phi_1^{-1/3} - 1)$. However, the most widely used bounds are those based on a variational principle first proposed by Hashin and Shtrikman (1962*a*,*b*). These are rigorous bounds involving no approximations other than those used in describing the microstructure of the material. For an isotropic two-phase composite in which the phases are individually homogenous and fully intermixed, the bounds derived by Hashin and Shtrikman (1963) apply

Bound 1:

$$K_{agg} = K_2 + \phi_1\{(K_1 - K_2)^{-1} + 3\phi_2(3K_2 + 4G_2)^{-1}\}^{-1} \quad (23a)$$

$$G_{agg} = G_2 + \phi_1\{(G_1 - G_2)^{-1} + 6\phi_2(K_2 + 2G_2)[5G_2(3K_2 + 4G_2)]^{-1}\}^{-1} \quad (23b)$$

Bound 2:

$$K_{agg} = K_1 + \phi_2\{(K_2 - K_1)^{-1} + 3\phi_1(3K_1 + 4G_1)^{-1}\}^{-1} \quad (23c)$$

$$G_{agg} = G_1 + \phi_2\{(G_2 - G_1)^{-1} + 6\phi_1(K_1 + 2G_1)[5G_1(3K_1 + 4G_1)]^{-1}\}^{-1} \quad (23d)$$

where the K are the bulk moduli and the G are the shear moduli of the indicated materials, and where, in each case

$$E_{agg} = 9K_{agg}G_{agg}/(3K_{agg} + G_{agg}) \quad (23e)$$

For materials of more complex microstructure, other formulations of the Hashin-Shtrikman bounds have been developed (Willis, 1981; Kantor and Bergman, 1984; Milton and Kohn, 1988), although the addition of the microstructural description requires that they be evaluated numerically.

Validation of the technique: the olivine + magnesiowüstite results

As an illustration of these data analysis procedures, and to demonstrate that the experimental technique gives good results, the olivine (ol) + magnesiowüstite (mw) results shown in Fig. 7 have been subjected to this analysis.

In Fig. 8 the olivine and magnesiowüstite phase average axial elastic strains at given applied differential stress are plotted against each other, and the best-fit curve given by A_{mw}/A_{ol} (see equation 18) is shown. Also shown are the bounds on the behaviour predicted by homogeneous stress (equation 18 using the E_{agg} given by equation 20) and homogeneous strain (equation 18 using the E_{agg} given by equation 21), where the phase properties used are given in Table 1. The neutron diffraction data fall between the homogeneous stress and homogeneous strain bounds as required, but the elastic properties of olivine and magnesiowüstite are sufficiently different for

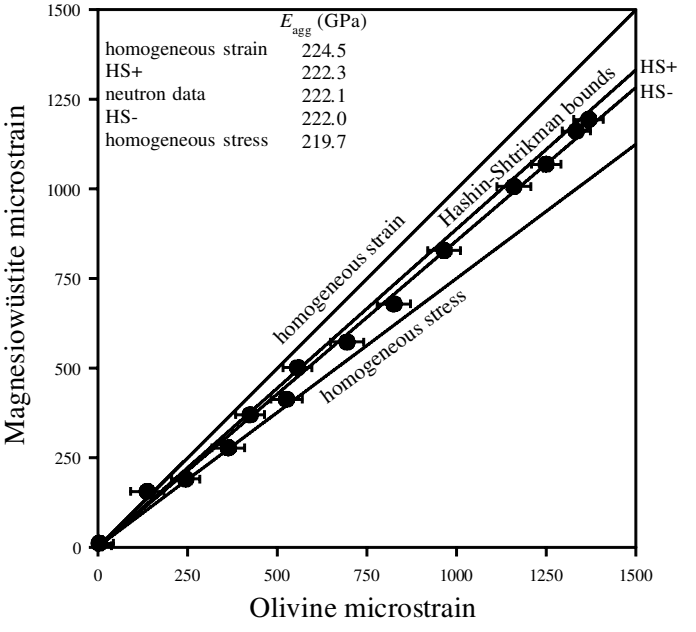

FIG. 8. The relationship between the phase average axial elastic strains of olivine and magnesiowüstite at given applied differential stress for the data shown in Fig. 7. Also shown are the theoretical bounds on the behaviour predicted by assuming homogeneous stress and homogeneous strain (equations 20 and 21), and the maximum and minimum bounds obtained using the Hashin-Shtrikman variational principle (equation 23). The neutron diffraction data not only fall between the homogeneous stress and homogeneous strain bounds as required, but also between the Hashin-Shtrikman bounds. This provides a strong confirmation of the validity of the technique.

these bounds to be quite widely separated, and so this, in itself, does not provide a very strong test of the technique. However, in contrast, the Hashin-Shtrikman bounds given by equation 18 are very closely spaced, and the experimental data fall between these two bounds providing a very strong validation of the technique. Indeed, to our knowledge, these results provide the first direct demonstration of the validity of the widely used Hashin-Shtrikman bounds, although the validity of these bounds has been demonstrated indirectly before (Watt and O'Connell, 1980) and is not in question.

The value of E_{agg} obtained using equation 19 is compared with various theoretical values given by equations 20, 21 and 23 in Fig. 8. The values of E_{agg} given by Ravichandran's bounds (equations 22*a* and 22*b*) are 222.3 GPa and 223.1 GPa, respectively. Setting equation 22*a* equal to equation 19, and solving the resulting

TABLE 1. Magnesiowüstite (mw) and olivine (ol) elastic properties (in GPa). $c_{ij} = c_{ji}$ are the non-zero components of the single-crystal elastic stiffness tensor for each phase (magnesiowüstite (mw) data from Jacobsen *et al*., 2002; olivine (ol) data from Webb *et al.*, 1989). K, G, E and ν are the bulk modulus, shear modulus, Young's modulus and Poisson's ratio, respectively, as obtained by isotropically averaging the single-crystal stiffnesses using the Hashin-Shtrikman scheme (Hashin and Shtrikman, 1962*b*; Watt, 1979).

	c_{11}	c_{12}	c_{13}	c_{22}	c_{23}	c_{33}	c_{44}	c_{55}	c_{66}	K	G	E	ν
mw	269.9	110.1	110.1	269.6	110.1	269.6	127.1	127.1	127.1	163.3	105.5	260.4	0.234
ol	320.2	67.9	70.5	195.9	78.5	233.8	63.5	76.9	78.1	129.5	77.54	193.9	0.250

quadratic for E_{mw} using the E_{ol} in Table 1 yields E_{mw} = 267.1 GPa, or if the quadratic is solved for E_{ol} using the E_{mw} in Table 1 then E_{ol} = 189.0 GPa. Alternatively, setting equation 22*b* equal to equation 19, and solving the resulting quadratic for E_{mw} using the E_{ol} in Table 1 yields E_{mw} = 316.8 GPa, or if the quadratic is solved for E_{ol} using the E_{mw} in Table 1 then E_{ol} = 159.4 GPa. In this case equation 22*a* yields results much more consistent with the published elastic properties of olivine and magnesiowüstite than does equation 22*b* (see Table 1). These manipulations show that when the elastic properties of the constituent phases are well established, as they are in this case, then the neutron diffraction data can indeed be a sensitive test of different theoretical treatments or, alternatively, if there is confidence in the theoretical treatment, that they can provide good estimates of the phase properties.

Applications of the technique

The results for the elastically isotropic olivine + magnesiowüstite sample described above, show that for such materials the technique can be used to test different theoretical methods of calculating composite properties from those of the constituent phases, even when the elastic property contrast between the mineral phases is not very large. Alternatively, if there is confidence in the theoretical method, then the technique may be used to determine the elastic properties of one of the phases when the other is known well. For composites in which the elastic property contrast between the constituent minerals is very large and hence the bounds on the composite properties are widely separated, the technique can be used to determine exactly where between the theoretical bounds the actual properties lie.

The technique, however, has a much more powerful application in the investigation of the factors which influence elastic anisotropy. Factors which are known to produce elastic property anisotropy in geological materials include: (1) the presence of a lattice-preferred orientation in one or more of the constituent mineral phases; (2) variations in the spatial distribution of the phases in the material (i.e. the extent to which there is mineralogical layering); (3) the presence of a grain-shape fabric; (4) spatial variations in grain size (if the grain boundaries have significantly different material properties than the grains themselves); and (5) the presence of oriented fractures/porosity. Since all these factors vary widely in natural materials, there is potentially much information to be recovered about the structure and composition of the Earth's interior from observations of seismic anisotropy, provided that a detailed quantitative understanding of the relative significance of each factor on the whole-rock anisotropy has been established. Unfortunately, it is generally difficult to investigate each of these factors independently using conventional rock mechanics techniques because in any suite of samples where one of the factors varies significantly, others tend to vary too. Moreover, experimental measurements on natural materials are almost invariably dominated by the effect of fractures/porosity unless the measurements are made at high confining pressures, where the technical complexity of the experiments compromises the quality of the data. The neutron diffraction experimental technique described above circumvents many of these problems. In providing lattice strain measurements rather than whole-rock properties, the data are relatively unaffected by the presence of fractures. Moreover, in providing information on the strain in different lattice directions, detailed grain-scale information of how strain (and hence stress) is partitioned between grains of different orientation can be obtained by carrying out experiments in which the loading direction is varied with respect to the geometry of the anisotropy. This allows the different schemes for calculating the elastic properties of anisotropic materials from, for example, observations of the lattice preferred orientations of the mineral phases in the rock, to be tested in a much more rigorous manner than they can be with whole rock property measurements. An initial attempt to do this for a strongly deformed olivine + orthopyroxene rock is described elsewhere (Covey-Crump *et al.*, 2003*a*), and further work examining the influence of variations in spatial distribution of the phases in olivine + magnesiowüstite composites is in progress.

A further important area of rock mechanics research where the experimental technique can provide important new information lies in the investigation of the plastic flow properties of geological materials (monomineralic or polymineralic), particularly at strains near the plastic yield point where the rate of change of properties with strain is at its greatest. Examination of changes in the relative strains in the different lattice directions with applied load provides

information about which slip systems are active. In polymineralic materials, changes in elastic strain partitioning between the constituent minerals during yielding provides important insight into the process of load transfer from the weaker to the stronger phases, a process which controls the yield behaviour of the whole rock. Preliminary experiments designed to investigate this matter in halite-bearing two-phase composites have been performed and are described elsewhere (Covey-Crump *et al.*, 2003*b*). The description of the constitutive properties of a plastically deforming material is a considerably more complex theoretical task than the equivalent elastic problem. Consequently, the type of information that can be recovered from deformation experiments conducted in the neutron beam-line is likely to play an important role in shaping the direction of future theoretical developments in this area.

The applications described above have focused upon the investigation of the mechanical properties of polycrystalline materials. However, the same type of test as described here may be used to determine the single crystal elastic stiffness tensor for a given phase from measurements made on polycrystalline samples of that phase (Howard and Kisi, 1999; Matthies *et al.*, 2001). This is particularly useful under circumstances where single crystals of the necessary size, purity, and shape are unavailable. In addition, the technique has considerable potential for determining the stresses required for mechanically-induced crystallographic/phase transformations, and thereby to improve greatly the calibrations of a number of piezometers which are used to estimate the differential stresses occurring during natural deformation. At present, such piezometers are calibrated by loading a series of nominally identical samples to different stresses and by then examining the experimental run products to determine the extent of the stress-induced transformation. Such calibrations are subject to specimen variability and to an uncertainty concerning at exactly what stress the features observed in the final microstructure were actually formed. By monitoring the progress of the transformation during the experiment, these problems are circumvented. Attempts to calibrate ferroelastic transformations in ceramics in this way have proved successful (e.g. Cain *et al.*, 1994), and work is currently in progress to recalibrate the calcite twinning piezometer.

The experimental technique described above involves experiments conducted at ambient pressures and temperatures. However, ENGIN has the capability of performing the same experiments at up to 1000°C. Attention is also being given to designing a pressure vessel which will allow the experiments to be performed at room temperature at confining pressures of up to 200 MPa.

Conclusions

An experimental method for investigating mechanical properties of geological materials using neutron diffraction techniques has been described. By carrying out deformation experiments in the neutron beam-line, the lattice parameters of all the mineral phases present in the sample may be determined as a function of differential load, and from this information the way in which deformation is partitioned between grains of different orientation and between different mineral phases may be examined. Such measurements permit a much closer examination of theoretical models of the mechanical behaviour of polycrystalline monomineralic and polymineralic materials than is possible from measurements of whole rock properties alone. Moreover, since the experiments can be performed on samples of similar size to those used in conventional rock mechanics tests, the high-quality information obtained from the neutron diffraction data need not be compromised by being combined with low-quality mechanical data. The technique requires a neutron facility which combines high flux, polychromatic neutrons with medium/high resolution powder diffractometers, such as is available on the ENGIN beam-line at the ISIS neutron spallation source, UK. With the imminent commissioning of ENGIN-X, the second-generation engineering beam-line at ISIS offering far greater flux, detector coverage, and resolution than is currently achievable on ENGIN, the range of mechanical problems which it is possible to address using the technique will be greatly extended.

Acknowledgements

The neutron beam-time at ISIS during which the techniques described above were developed, was funded by the Natural Environment Research Council (NERC) through the Central Laboratory of the Research Councils, UK, and by NERC research grant (GR9/04331). The work was carried out while SJCC held a Royal Society University Research Fellowship.

References

Birch, J.M., Wilshire, B., Owen, D.J.R. and Shantaram, D. (1976) The influence of stress distribution on the deformation and fracture behaviour of ceramic materials under compression creep conditions. *Journal of Materials Science*, **11**, 1817–1825.

Bloomfield, J.P. and Covey-Crump, S.J. (1993) Correlating mechanical data with microstructural observations in deformation experiments on synthetic two-phase aggregates. *Journal of Structural Geology*, **15**, 1007–1019.

Cain, M.G., Bennington, S.M., Lewis, M.H. and Hull, S. (1994) Study of the ferroelastic transformation in zirconia by neutron diffraction. *Philosophical Magazine B*, **69**, 499–507.

Carter, D.H. and Bourke, M.A.M. (2000) Neutron diffraction study of the deformation behaviour of beryllium-aluminum composites. *Acta Materialia*, **48**, 2885–2900.

Clausen, B. (1997) *Characterisation of Polycrystal Deformation by Numerical Modelling and Neutron Diffraction Experiments*. PhD Thesis, Risø National Laboratory, Roskilde, Denmark.

Clyne, T.W. and Withers, P.J. (1993) *An Introduction to Metal Matrix Composites*. Cambridge University Press, UK, 509 pp.

Covey-Crump, S.J., Schofield, P.F. and Stretton, I.C. (2001) Strain partitioning during the elastic deformation of an olivine + magnesiowüstite aggregate. *Geophysical Research Letters*, **28**, 4647–4650.

Covey-Crump, S.J., Schofield, P.F., Stretton, I.C., Knight, K.S. and Ben Ismaïl, W. (2003*a*) Using neutron diffraction to investigate the elastic properties of anisotropic rocks: results from an olivine + orthopyroxene mylonite. *Journal of Geophysical Research*, **108(B2)**, 2092, doi 10.1029/2002JB001816.

Covey-Crump, S.J., Schofield, P.F., Stretton, I.C., Daymond, M.R. and Knight, K.S. (2003*b*) Strain partitioning between the constituent phases during the plastic yielding of two-phase composites. In preparation for submission to *Acta Materialia*.

Cropper, D.R. and Pask, J.A. (1969) Effect of plastic instability on compressive deformation. *American Ceramic Society Bulletin*, **48**, 555–558.

Daymond, M.R. (2001) The blurring in strains measured at a pulsed neutron source introduced by the use of a detector with a large angular coverage. *Physica B*, **301**, 221–226.

Daymond, M.R. and Priesmeyer, H.G. (2002) Elastoplastic deformation of ferritic steel and cementite studied by neutron diffraction and self-consistent modelling. *Acta Materialia*, **50**, 1613–1626.

Daymond, M.R., Bourke, M.A.M., Von Dreele, R.B., Clausen, B. and Lorentzen, T. (1997) Use of Rietveld refinement for elastic macrostrain determination and for evaluation of plastic strain history from neutron diffraction spectra. *Journal of Applied Physics*, **82**, 1554–1562.

Daymond, M.R., Bourke, M.A.M. and Von Dreele, R.B. (1999*a*) Use of Rietveld refinement to fit a hexagonal crystal lattice in the presence of elastic and plastic anisotropy. *Journal of Applied Physics*, **85**, 739–747.

Daymond, M.R., Lund, C., Bourke, M.A.M and Dunand, D.C. (1999*b*) Elastic phase-strain distribution in a particulate reinforced metal-matrix composite deforming by slip or creep. *Metallurgical Materials Transactions A*, **30**, 2989–2997.

Dunand, D.C., Mari, D., Bourke, M.A.M. and Roberts, J.A. (1996) NiTi and NiTi-TiC composites: part IV. Neutron diffraction study of twinning and shape-memory recovery. *Metallurgical Materials Transactions A*, **27**, 2820–2836.

Fan, Z. and Miodownik, A.P. (1993) The deformation behaviour of alloys comprising two ductile phases – I. Deformation theory. *Acta Metallurgica et Materialia*, **41**, 2403–2413.

Frischbutter, A., Neov, D., Scheffzück, Ch., Vrána, M. and Walther, K. (2000) Lattice strain measurements on sandstones under load using neutron diffraction. *Journal of Structural Geology*, **22**, 1587–1600.

Hashin, Z. (1983) Analysis of composite materials – a survey. *Journal of Applied Mechanics*, **50**, 481–505.

Hashin, Z. and Shtrikman, S. (1962*a*) On some variational principles in anisotropic and nonhomogeneous elasticity. *Journal of the Mechanics and Physics of Solids*, **10**, 335–342.

Hashin, Z. and Shtrikman, S. (1962*b*) A variational approach to the theory of the elastic behaviour of polycrystals. *Journal of the Mechanics and Physics of Solids*, **10**, 343–352.

Hashin, Z. and Shtrikman, S. (1963) A variational approach to the elastic behaviour of multiphase materials. *Journal of the Mechanics and Physics of Solids*, **11**, 127–140.

Hill, R. (1952) The elastic behaviour of a crystalline aggregate. *Proceedings of the Physical Society of London A*, **65**, 349–354.

Hill, R. (1963) Elastic properties of reinforced solids: some theoretical principles. *Journal of the Mechanics and Physics of Solids*, **11**, 357–372.

Howard, C.J. and Kisi, E.H. (1999) Measurement of single-crystal elastic constants by neutron diffraction from polycrystals. *Journal of Applied Crystallography*, **32**, 624–633.

Jacobsen, S.D., Reichmann, H.-J., Spetzler, H.A., Mackwell, S.J., Smyth, J.R., Angel, R.J. and McCammon, C.A. (2002) Structure and elasticity

of single-crystal (Mg,Fe)O and a new method of generating gigaherz ultrasonic interferometry. *Journal of Geophysical Research*, **107(B2)**, 2037, doi 10.129/2001JB000490.

Johnson, M.W. (1988) Data Acquisition. Pp. 127–143 in: *Neutron Scattering at a Pulsed Source* (R.J. Newport, B.D. Rainford and R. Cywinski, editors). Adam Hilger Publishers, Bristol, UK.

Johnson, M.W. and Daymond, M.R. (2002) An optimum design for a time-of-flight neutron diffractometer for measuring engineering stresses. *Journal of Applied Crystallography*, **35**, 49–57.

Johnson, M.W., Edwards, L. and Withers, P.J. (1997) ENGIN – a new instrument for engineers. *Physica B*, **234–236**, 1141–1143.

Kantor, Y. and Bergman, D.J. (1984) Improved rigorous bounds on the effective elastic moduli of a composite material. *Journal of the Mechanics and Physics of Solids*, **32**, 41–62.

Larson, A.C. and Von Dreele, R.B. (1994) *General Structure Analysis System (GSAS)*. Los Alamos National Laboratory Report, LAUR 86-748 (revised version), New Mexico, USA, 223 pp.

MacEwen, S.R., Faber Jr., J. and Turner, A.P.L. (1983) The use of time-of-flight neutron diffraction to study grain interaction stresses. *Acta Metallurgica*, **31**, 657–676.

Majumdar, S., Singh, J.P., Kupperman, D. and Krawitz, A.D. (1991) Application of neutron diffraction to measure residual strains in various engineering composite materials. *Journal of Engineering Materials Technology*, **113**, 51–59.

Matthies, S., Priesmeyer, H.G. and Daymond, M.R. (2001) On the diffractive determination of single-crystal elastic constants using polycrystalline samples. *Journal of Applied Crystallography*, **34**, 585–601.

Mecking, H. and Dunst, D. (1994) Microstructural interactions during flow of two-phase titanium alloys. *Materials Science Engineering*, **A175**, 55–62.

Meredith, P.G., Wood, I.G., Knight, K.S. and Boon, S.A. (1997) In-situ measurement of strain partitioning during rock deformation by neutron diffraction imaging. *Journal of Conference Abstracts*, **2**, 50.

Meredith, P.G., Knight, K.S., Boon, S.A. and Wood, I.G. (2001) The microscopic origin of thermal cracking in rocks: an investigation by simultaneous time-of-flight neutron diffraction and acoustic emission monitoring. *Geophysical Research Letters*, **28**, 2105–2108.

Milton, G.W. and Kohn, R.V. (1988) Variational bounds on the effective moduli of anisotropic composites. *Journal of the Mechanics and Physics of Solids*, **36**, 597–629.

Nemat-Nasser, S. and Hori, M. (1999) *Micromechanics: Overall Properties of Heterogeneous Materials* (2nd edition), Elsevier, Amsterdam, 786 pp.

Paul, B. (1960) Prediction of the elastic constants of multiphase materials. *Transactions of the Metallurgical Society of the AIME*, **218**, 36–41.

Pintschovius, L., Prem, M. and Frischbutter, A. (2000) High-precision neutron-diffraction measurements for the determination of low-level residual stresses in a sandstone. *Journal of Structural Geology*, **22**, 1581–1585.

Ponte Castañeda, P. and Suquet, P. (1998) Nonlinear composites. *Advanced Applied Mechanics*, **34**, 171–302.

Ravichandran, K.S. (1994) Elastic properties of two-phase composites. *Journal of the American Ceramics Society*, **77**, 1178–1184.

Schäfer, W. (2002) Neutron diffraction applied to geological texture and stress analysis. *European Journal of Mineralogy*, **14**, 263–289.

Scheffzük, Ch., Frischbutter, A., and Walther, K. (1998) Intracrystalline strain measurements with time-of-flight neutron diffraction: application to a Cretaceous sandstone from the Elbezone (Germany). *Schriftenreihe für Geowissenschaften*, **6**, 39–48.

Sears, V.F. (1992) Neutron scattering lengths and cross sections. *Neutron News* **3**, 26–37.

Watt, J.P. (1979) Hashin-Shtrikman bounds on the effective elastic moduli of polycrystals with orthorhombic symmetry. *Journal of Applied Physics*, **50**, 6290–6295.

Watt, J.P. and O'Connell, R.J. (1980) An experimental investigation of the Hashin-Shtrikman bounds on two-phase aggregate elastic properties. *Physics of the Earth and Planetary Interior,* **21**, 359–370.

Watt, J.P., Davies, G.F. and O'Connell, R.J. (1976) The elastic properties of composite materials. *Reviews in Geophysics and Space Physics*, **14**, 541–563.

Webb, S.L. (1989) The elasticity of the upper mantle orthosilicates olivine and garnet to 3 Gpa. *Physics and Chemistry of Minerals*, **16**, 684–692.

Webster, G.A. and Ezeilo, A.N. (1997) Neutron scattering in engineering applications. *Physica B*, **234**, 949–955.

Wenk, H.-R. (1998) Pole figure measurements with diffraction techniques. Pp. 126–177 in: *Texture and Anisotropy* (U.F. Kocks, C.N. Tomé and H.-R. Wenk, editors). Cambridge University Press, UK.

Willis, J.R. (1981) Variational and related methods for the overall properties of composites. *Advanced Applied Mechanics*, **21**, 1–78.

Wilson, C.C. (1995) A guided tour of ISIS – the UK neutron spallation source. *Neutron News*, **6**, 27–34.

Withers, P.J., Daymond, M.R. and Johnson, M.W. (2001) The accuracy of diffraction peak location.

Journal of Applied Crystallography, **34**, 737–743.

Young, R.A. (1993) Introduction to the Rietveld method. Pp. 1–38 in: *The Rietveld Method* (R.A. Young, editor). Oxford University Press, Oxford, UK.

Zhao, P. and Ji, S. (1997) Refinements of shear-lag model and its applications. *Tectonophysics*, **279**, 37–53.

Zheng, Q.-S. and Du, D.-X. (2001) An explicit and universally applicable estimate for the effective properties of multiphase composites which accounts for inclusion distribution. *Journal of the Mechanics and Physics of Solids*, **49**, 2765–2788.

[*Manuscript received 15 July 2002: revised 10 December 2002*]